

Filling a Void: Isolation and Characterization of Tetracarboxylato Dimolybdenum Cations

F. Albert Cotton,^{*,†} Lee M. Daniels,[†] Elizabeth A. Hillard,[†] and Carlos A. Murillo^{*,†,‡}

Department of Chemistry and Laboratory for Molecular Structure and Bonding, P.O. Box 30012, Texas A&M University, College Station, Texas 77842-3012, and Department of Chemistry, University of Costa Rica, Ciudad Universitaria, Costa Rica

Received October 18, 2001

Dimolybdenum tetracarboxylato cations have been prepared and structurally characterized for the first time. The reactions of the new, quadruply bonded compound, $\text{Mo}_2(\text{TiPB})_4$, where $\text{TiPB} = 2,4,6$ -triisopropylphenyl carboxylate, with NOPF_6 and NOBF_4 give the ionic compounds $[\text{Mo}_2(\text{TiPB})_4]\text{PF}_6$ and $[\text{Mo}_2(\text{TiPB})_4]\text{BF}_4$, respectively. Each product crystallizes in space group $P2_1/n$ and displays an elongation of the Mo–Mo bond of 0.060 and 0.068 Å, respectively, over that of the parent compound (2.076(1) Å). Each complex displays a characteristic EPR signal, showing hyperfine coupling to the spin active isotopes ^{95}Mo and ^{97}Mo , with $g_{\parallel} = g_{\perp} = 1.936$, that is consistent with the presence of an unpaired electron. Electronic spectroscopy indicates the expected red shift in the $\delta \rightarrow \delta^*$ transition for the cations, due to the loss of exchange energy in going from the two-electron to one-electron system. We have also obtained a small amount of crystalline $[\text{Mo}_2(\text{O}_2\text{CC}_4\text{H}_9)_4]\text{PF}_6$ from the reaction of $\text{Mo}_2(\text{O}_2\text{CC}_4\text{H}_9)_4$ with AgPF_6 . This product crystallizes in the space group $C2/c$, and the Mo–Mo bond is elongated by 0.063 Å over that of the neutral parent compound. These ionic compounds have the first isolated and characterized $[\text{Mo}_2(\text{O}_2\text{CR})_4]^+$ cationic species.

Introduction

Among the thousands of M_2^{n+} compounds¹ the most numerous are those of Mo_2^{4+} . The earliest of the Mo_2^{4+} compounds to have been reported² and then structurally characterized³ were those of the paddlewheel tetracarboxylato type, $\text{Mo}_2(\text{O}_2\text{CR})_4$. These were also among the earliest M_2^{n+} compounds to be subjected to rigorous molecular orbital calculations,⁴ detailed electronic spectroscopic study,⁵ and photoelectron spectroscopic⁶ study. It is, therefore, surprising to note how little is known about their redox chemistry.⁷

* Authors to whom correspondence should be addressed. E-mail: cotton@tamu.edu (F.A.C.); murillo@tamu.edu (C.A.M.).

† University of Costa Rica.

‡ Texas A&M University.

- (1) Cotton, F. A.; Walton, R. A. *Multiple Bonds Between Metal Atoms*, 2nd ed.; Oxford University Press: Oxford, 1993.
- (2) (a) Abel, E. W.; Singh, A.; Wilkinson, G. *J. Am. Chem. Soc.* **1959**, *81*, 3097. (b) Bannister, E.; Wilkinson, G. *Chem. Ind. (London)* **1960**, 319. (c) Stephenson, T. A.; Bannister, E.; Wilkinson, G. *J. Am. Chem. Soc.* **1963**, *85*, 6012.
- (3) (a) Lawton, D.; Mason, R. *J. Am. Chem. Soc.* **1965**, *87*, 921. (b) Cotton, F. A.; Mester, Z. C.; Webb, T. R. *Acta Crystallogr.* **1974**, *B30*, 2768.
- (4) Norman, J. G., Jr.; Kolari, H. J. *J. Chem. Soc., Chem. Commun.* **1975**, 649.
- (5) Cotton, F. A.; Zhong, B. *J. Am. Chem. Soc.* **1990**, *112*, 2256 and references therein.

Even more surprising is the fact that although the limited electrochemical data show that reversible (or at least quasi-reversible) oxidation to $\text{Mo}_2(\text{O}_2\text{CR})_4^+$ ions occurs at potentials well below +1.0 V,⁸ no such species has ever been structurally characterized over the approximately 40 year period since the $\text{Mo}_2(\text{O}_2\text{CR})_4$ compounds were discovered.

We now report that the gap has been filled by the preparation of $[\text{Mo}_2(\text{TiPB})_4]\text{PF}_6 \cdot 2\text{CH}_2\text{Cl}_2$, **1**· $2\text{CH}_2\text{Cl}_2$, and $[\text{Mo}_2(\text{TiPB})_4]\text{BF}_4 \cdot 2\text{CH}_2\text{Cl}_2$, **2**· $2\text{CH}_2\text{Cl}_2$, where TiPB is 2,4,6-triisopropylphenyl carboxylate, and their detailed structural and physical characterization. For comparison, we also report on the parent compound $\text{Mo}_2(\text{TiPB})_4$, **3**, and the structure of the pivalato cation in $[\text{Mo}_2(\text{O}_2\text{CC}_4\text{H}_9)_4]\text{PF}_6$, **4**.

Experimental Section

General Procedures. All manipulations were carried out in an inert atmosphere utilizing standard Schlenk and drybox techniques. All reagents and solvents were obtained commercially. Anhydrous

- (6) Lichtenberger, D. L.; Johnston, R. L. In *Metal-Metal Bonds and Clusters in Chemistry and Catalysis*; J. P. Fackler, Jr., Ed.; Plenum Press: New York, 1990.
- (7) Reference 1, pp 161–162.
- (8) For a recent reference, see: Liworncharoenvong, T.; Luck, R. L. *J. Am. Chem. Soc.* **2001**, *123*, 3615.

Table 1. Crystallographic Data for [Mo₂(O₂CR)₄]⁰⁺ Complexes

	1·2CH ₂ Cl ₂	2·2CH ₂ Cl ₂	3	4
empirical formula	C ₆₆ H ₉₆ Cl ₄ F ₆ Mo ₂ O ₈ P	C ₆₆ H ₉₆ Cl ₄ F ₄ Mo ₂ O ₈ B	C ₆₄ H ₉₂ Mo ₂ O ₈	C ₂₀ H ₃₆ F ₆ Mo ₂ O ₈ P
fw	1496.08	1437.92	1181.26	741.34
space group	P2 ₁ /n (No. 14)	P2 ₁ /n (No. 14)	P $\bar{1}$ (No. 2)	C2/c (No. 15)
a, Å	9.4884(6)	9.2621(7)	9.709(6)	16.764(4)
b, Å	18.757(1)	18.755(2)	12.035(8)	10.454(2)
c, Å	20.428(1)	20.510(2)	14.574(6)	19.246(4)
α, deg	90	90	100.01(4)	90
β, deg	98.319(2)	98.210(2)	107.95(3)	115.351(3)
γ, deg	90	90	103.36(6)	90
V, Å ³	3597.4(4)	3526.3(4)	1520(2)	3048(1)
Z	2	2	1	4
T, °C	−60	−60	−60	−60
λ, Å	0.71073	0.71073	0.71073	0.71073
d _{calcd.} , g/cm ³	1.381	1.354	1.290	1.615
μ, mm ^{−1}	0.584	0.567	0.464	0.949
R1 ^a (wR2 ^b)	0.1354 (0.1423)	0.0709 (0.0808)	0.0689 (0.1713)	0.0330 (0.0765)

$${}^a R1 = \sum ||F_o| - |F_c|| / \sum |F_o|. \quad {}^b wR2 = [\sum [w(F_o^2 - F_c^2)^2] / \sum [w(F_o^2)^2]]^{1/2}, \quad w = 1/[\sigma^2(F_o^2) + (aP)^2 + bP], \quad \text{where } P = [\max(F_o^2 \text{ or } 0) + 2(F_c^2)]/3.$$

dichlorobenzene was purchased from Aldrich Chemical Company in Sure-Seal bottles. Dichloromethane was dried over P₂O₅, hexanes and toluene over Na/K alloy, and these solvents were freshly distilled under N₂ prior to use.

Physical Measurements. Elemental analyses were performed by Canadian Microanalytical Service, Ltd., Delta, British Columbia, Canada. ¹H NMR spectra were recorded on a Unity Plus 300 NMR spectrometer, with chemical shifts (δ) referenced to CH₂Cl₂. The cyclic voltammograms were recorded on a BAS 100 electrochemical analyzer in 0.1 M Buⁿ₄NPF₆ solutions with Pt working and auxiliary electrodes and a Ag/AgCl reference electrode; scan rates were 100 mV s^{−1} in all cases. The EPR spectra were recorded on a Bruker ESP300 spectrometer. The magnetic susceptibility measurements were recorded on a Quantum Design SQUID MPMS-XL magnetometer. UV/vis spectra were recorded on a Cary 17D spectrophotometer.

X-ray Crystallography. Single crystals of 1·2CH₂Cl₂, 2·2CH₂Cl₂, and 4 were attached to glass fibers with a small amount of silicon grease and mounted on the Bruker SMART system for data collection using Mo Kα radiation at 213(2) K. Single-crystal X-ray work on 3 was performed on a Nonius FAST diffractometer utilizing the program MADNES with Mo Kα radiation at 213(2) K. Cell parameters were obtained from an autoindexing routine. For 1·2CH₂Cl₂, cell parameters were refined with 3118 reflections within a 2θ range of 4.324–51.07°. For 2·2CH₂Cl₂, cell parameters were refined with 5034 reflections within a 2θ range of 4.554–54.975°. For 3, cell parameters were refined with 250 reflections within a 2θ range of 18.2–41.6°. For 4, cell parameters were refined with 6400 reflections within a 2θ range of 4.684–54.98°.

For all compounds, the coordinates of some or all of the non-hydrogen atoms were found via direct methods using the structure solution program SHELXS.⁹ The positions of the remaining non-hydrogen atoms were located by use of a combination of least-squares refinement and difference Fourier maps in the SHELXL-93 program.¹⁰ Non-hydrogen atoms were refined with anisotropic displacement parameters, except for disordered portions of the structures (isopropyl groups in 1·2CH₂Cl₂, fluorine atoms in 2·2CH₂Cl₂, phenyl rings and isopropyl groups in 3, and *tert*-butyl groups in 4). The hydrogen atoms were included in the structure factor calculations at idealized positions. Cell parameters and

Table 2. Selected Bond Lengths (Å) and Angles (deg) for [Mo₂(O₂CR)₄]⁰⁺ Complexes

	1·2CH ₂ Cl ₂	2·2CH ₂ Cl ₂	3	4
Mo(1)–Mo(1a) ^a	2.1364(8)	2.1441(5)	2.076(1)	2.1512(5)
Mo(1)–O(1)	2.074(3)	2.071(2)	2.084(4)	2.079(2)
Mo(1)–O(2)	2.066(3)	2.070(1)	2.113(4)	2.080(2)
Mo(1)–O(3)	2.063(3)	2.065(2)	2.084(4)	2.073(2)
Mo(1)–O(4)	2.062(3)	2.065(1)	2.088(4)	2.077(2)
Mo(1a)–Mo(1)–O(1)	91.70(9)	91.54(5)	92.8(1)	91.31(5)
Mo(1a)–Mo(1)–O(2)	91.67(8)	91.64(4)	90.9(1)	91.04(5)
Mo(1a)–Mo(1)–O(3)	90.6(1)	90.71(5)	91.4(1)	91.25(5)
Mo(1a)–Mo(1)–O(4)	90.57(9)	90.61(5)	92.0(1)	91.04(5)
<i>cis</i> -O–Mo(1)–O	90.0[1]	89.98[6]	89.9[2]	89.98[8]
<i>trans</i> -O–Mo(1)–O	176.7[1]	176.96[6]	176.1[1]	177.67[6]

^a Mo(1) and Mo(1a) are related by an inversion center in all compounds.

refinement results for all compounds are summarized in Table 1. Selected bond distances and angles are given in Table 2.

In 2·2CH₂Cl₂, the BF₄[−] group resides on the inversion center halfway between the dinuclear Mo centers, located directly in line with the axial positions. The anion was modeled as a rigid tetrahedron, and further refinement followed by examination of difference Fourier maps revealed at least two other orientations in addition to the disorder imposed by the site symmetry. Therefore three BF₄[−] units were included at the site as rigid tetrahedra in which the B–F bonds were allowed to shrink or expand. The B atoms were not constrained to remain exactly on the inversion center. The sum of the occupancies was constrained to equal full occupancy for the site, and one common isotropic displacement factor was refined for all F atoms and another for all B atoms. The final occupancies for the three orientations converged to 36.57(2)%, 31.06(2)%, and 32.37(2)%.

Preparation of [Mo₂(TiPB)₄]PF₆·2CH₂Cl₂, 1·2CH₂Cl₂. Mo₂-(TiPB)₄ (300 mg, 0.254 mmol) and NOPF₆ (45.0 mg, 0.257 mmol) were each combined with 20 mL of CH₂Cl₂. The yellow solution was transferred to a flask containing the NOPF₆ suspension, quickly affording a purple solution, which was stirred for 2 h. The mixture was filtered over Celite to remove any unreacted NOPF₆ and concentrated to about 10 mL. Red needles of 1·2CH₂Cl₂ suitable for X-ray structural analysis were grown after 24 h from the slow diffusion of hexanes into the filtrate. The yield was 0.060 g (52%). After elimination of interstitial solvent molecules under vacuum: Anal. for C₆₄H₉₂Mo₂O₈PF₆. Calcd (found): C, 57.97 (57.51); H, 6.99 (6.84). IR (KBr): 2964, 2931, 2870, 1700, 1687, 1655, 1638, 1605, 1561, 1543, 1460, 1403, 1320, 1284, 1262, 1156, 1107, 1087 cm^{−1}.

(9) Sheldrick, G. M. SHELXS, program for crystal structure solution. *Acta Crystallogr.* **1990**, *A46*, 467.

(10) Sheldrick, G. M. In *Crystallographic Computing 6*; Flack, H. D., Parkanyi, L., Simon, K., Eds.; Oxford University Press: Oxford, U.K., 1993; p 111.

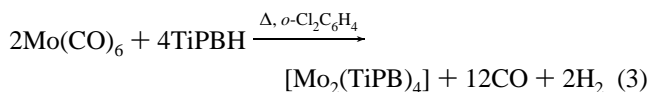
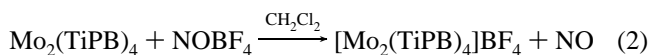
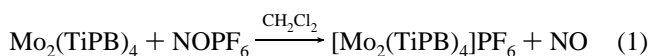
$[\text{Mo}_2(\text{TiPB})_4]\text{BF}_4 \cdot 2\text{CH}_2\text{Cl}_2, 2 \cdot 2\text{CH}_2\text{Cl}_2$. The corresponding BF_4 salt of $\text{Mo}_2(\text{TiPB})_4$ was prepared similarly, in comparable yield. After elimination of interstitial solvent molecules: Anal. for $\text{C}_{64}\text{H}_{92}\text{Mo}_2\text{O}_8\text{BF}_4$. Calcd (found): C, 60.62 (60.02); H, 7.31 (7.25). IR (KBr): 2963, 2930, 2870, 1701, 1686, 1655, 1637, 1605, 1562, 1544, 1460, 1403, 1320, 1292, 1261, 1194, 1156, 1108, 1089, 1052 cm^{-1} .

$\text{Mo}_2(\text{TiPB})_4, 3$. A mixture of $\text{Mo}(\text{CO})_6$ (2.640 g, 10.00 mmol) and HTiPB (4.977 g, 20.04 mmol) in 25 mL of *o*-dichlorobenzene was refluxed under N_2 for 4 days. Upon cooling, copious yellow solid was afforded, which was filtered and recrystallized by slow diffusion of hexanes into a hot, saturated toluene solution. The yield, before recrystallization, was essentially quantitative. Crystals suitable for X-ray crystallography were prepared by diffusion of hexanes into a saturated toluene solution of the product. Anal. for $\text{C}_{64}\text{H}_{92}\text{Mo}_2\text{O}_8$. Calcd (found): C, 65.08 (64.62); H, 7.85 (7.94). ^1H NMR δ (ppm, in CD_2Cl_2): 7.129 (s, 8 H, aromatic), 3.354 (septet, 8 H, *o*-isopropyl), 2.932 (septet, 4 H, *p*-isopropyl), 1.272 (doublet, 24 H, methyl), 1.175 (doublet, 48 H, methyl). IR (KBr): 2960, 2933, 2870, 1698, 1605, 1564, 1484, 1464, 1411, 1387, 1360, 1318, 1297, 1259, 1242, 1195, 1158, 1105, 1071, 1054 cm^{-1} .

$[\text{Mo}_2(\text{O}_2\text{CC}_4\text{H}_9)_4]\text{PF}_6, 4$. $\text{Mo}_2(\text{O}_2\text{CC}_4\text{H}_9)_4$ (200 mg, 0.335 mmol), prepared from a literature procedure,¹¹ and AgPF_6 (85.0 mg, 0.335 mmol) were dissolved in 20 and 5 mL of CH_2Cl_2 , respectively. Upon addition of the molybdenum solution to the flask containing the AgPF_6 solution, a green solution and black precipitate (Ag) quickly formed. The mixture was stirred for 1 h and then filtered over Celite. A few green blocks of **4** suitable for X-ray structural analysis were grown after 24 h from the slow diffusion of hexanes into the filtrate. Besides the few crystals, copious yellow and brown solids precipitated out of solution.

Results and Discussion

Compounds **1**, **2**, and **3** were synthesized by the following reactions:



The neutral, quadruply bonded $\text{Mo}_2(\text{TiPB})_4$ was obtained in excellent yield by the classical route. It displays a brilliant canary yellow color typical of other $\text{Mo}_2(\text{O}_2\text{CR})_4$ compounds. However, it is slightly more air sensitive than $\text{Mo}_2(\text{O}_2\text{CCH}_3)_4$, and the crystals turn greenish brown after several hours of exposure to the atmosphere. It is far more soluble in hexanes, toluene, ether, and dichloromethane than $\text{Mo}_2(\text{O}_2\text{CCH}_3)_4$ or $\text{Mo}_2(\text{O}_2\text{CC}_4\text{H}_9)_4$. This increased solubility makes recrystallization difficult, and crystals can be obtained only when a highly saturated solution of hot toluene is layered with hexanes. The solubility of the compound even in hexanes reduces the yields for the crystalline material; the extreme solubility of the compound in dichloromethane precludes crystallization from this solvent.

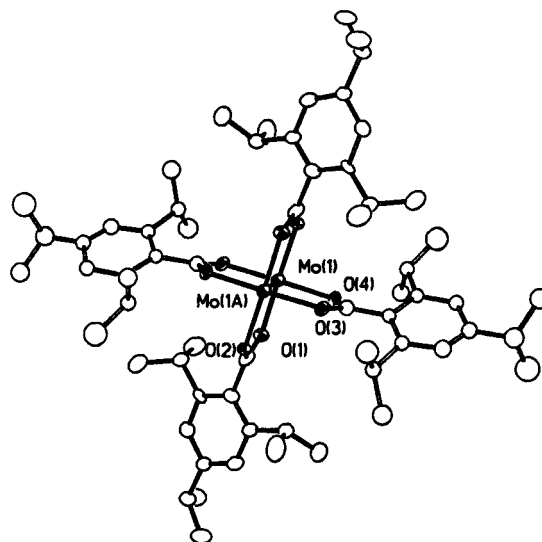


Figure 1. Thermal ellipsoid plot of tetrakis(2,4,6-triisopropylbenzoato)-dimolybdenum(II), **3**. Probability ellipsoids are shown at the 50% level. Hydrogen atoms and disordered phenyl and isopropyl groups of minor occupancy have been omitted for clarity.

The paramagnetic cationic species, $[\text{Mo}_2(\text{TiPB})_4]\text{PF}_6$, is deep red, while the BF_4 salt is somewhat more orange in color. These complexes are quite soluble and stable in dichloromethane, but completely insoluble in hexanes, thus contributing to the ease of preparation and crystallization. These solids are moderately air stable and decompose after about an hour in air, when they turn from red to brown. However, solutions of these complexes are extremely air-sensitive and lose all color within a couple of minutes in air. This process has also been observed via UV/vis spectroscopy, where all transitions in the visible range disappear after air exposure.

In **3**, the four carboxylate groups bridge the quadruply bonded Mo_2^{4+} unit, giving the typical paddlewheel arrangement shown in Figure 1. The Mo–Mo distance of 2.076(1) Å is marginally shorter by ca. 0.02 Å than that of most of the previously reported quadruply bonded $\text{Mo}_2(\text{O}_2\text{CR})_4$ compounds,¹ and the structure is similar to that of the chromium analogue.¹²

For the oxidized species, shown in Figures 2 and 3, the structure of the cation is generally similar, but the Mo–Mo separation, 2.1364(8) Å in **1** and 2.1441(5) Å in **2**, is significantly greater than that of the unoxidized starting material (2.076(1) Å). Thus, removal of one electron, which reduces the Mo–Mo bond order to 3.5, increases the distance by about 0.06–0.07 Å relative to that in the parent compound. The magnitude of the change in going from the $\sigma^2\pi^4\delta^2$ to the $\sigma^2\pi^4\delta$ configuration is typical for such a change, as may be seen by comparison with those for the pairs, $\text{Mo}_2(\text{SO}_4)_4^{4-}$ ¹³ and $\text{Mo}_2(\text{SO}_4)_4^{3-}$,¹⁴ with Mo–Mo distances of 2.110(2) and 2.164(2) Å, respectively, and for $\text{Mo}_2(\text{hpp})_4$ ¹⁵ and $[\text{Mo}_2(\text{hpp})_4]^+$ ¹⁶ (where hpp is the anion of 1,3,4,6,7,8-hexahydro-2H-pyrimido[1,2-*a*]pyrimidine), where the bond

(12) Cotton, F. A.; Hillard, E. A.; Murillo, C. A.; Zhou, H.-C. *J. Am. Chem. Soc.* **2000**, *122*, 416.

(13) Angell, C. L.; Cotton, F. A.; Frenz, B. A.; Webb, T. R. *J. Chem. Soc., Chem. Commun.* **1973**, 399.

(11) Stephenson, T. A.; Bannister, E.; Wilkinson, G. *J. Chem. Soc.* **1964**, 2538.

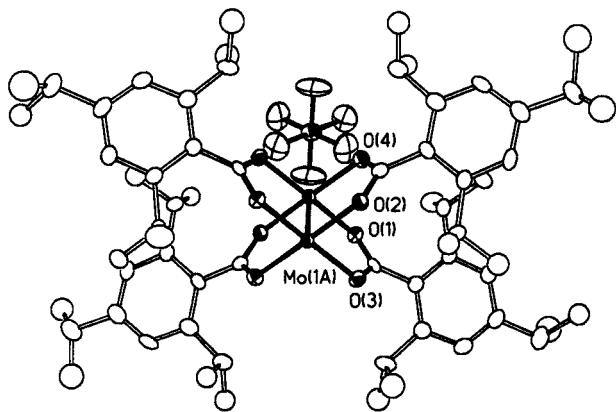


Figure 2. Thermal ellipsoid plot of the tetrakis(2,4,6-triisopropylbenzoato)-dimolybdenum(II,III) cation and PF_6^- anion in $1 \cdot 2\text{CH}_2\text{Cl}_2$. Probability ellipsoids are shown at the 50% level. Hydrogen atoms, solvent of crystallization, disordered isopropyl groups, and disordered fluorine atoms of minor occupancy have been omitted for clarity.

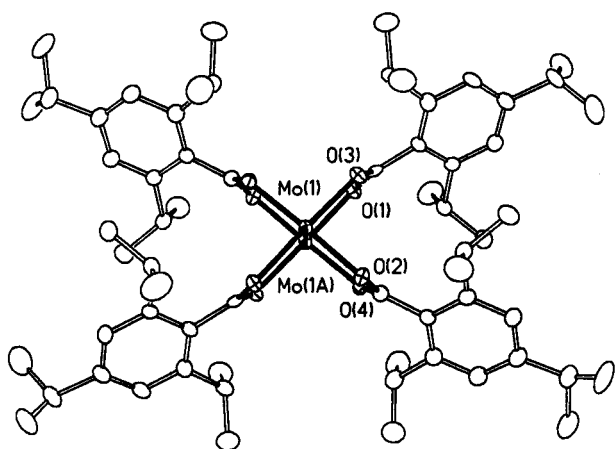


Figure 3. Thermal ellipsoid plot of the tetrakis(2,4,6-triisopropylbenzoato)-dimolybdenum(II,III) cation in $2 \cdot 2\text{CH}_2\text{Cl}_2$. Probability ellipsoids are shown at the 50% level. Hydrogen atoms, solvent of crystallization, and disordered tetrafluoroborate anion have been omitted for clarity.

distances are 2.067(1) and 2.127 Å, respectively. However, the change in the Mo–Mo distances is significantly smaller upon oxidation of $\text{Mo}_2[\mu-\eta-(\text{NPh})_2\text{CNHPh}]_4$, being only 2.0839(9)¹⁷ to 2.1194(12)¹⁸ (0.0355 Å). Furthermore, the increase in charge on the Mo_2 core from the loss of one electron causes the Mo–O bonds in the cations to contract by ca. 0.025 Å relative to the neutral parent compound.

The one-electron electrochemical oxidation ($\text{Mo}_2^{4+}/\text{Mo}_2^{5+}$) of **3** in dichloromethane, ethanol, and acetonitrile exhibits values for $E_{1/2}$ of +0.621, +0.448, and +0.462 V (vs Ag/AgCl), respectively. A representative cyclic voltammogram is depicted in Figure 4. While the trend is the same as that reported for solutions of $\text{Mo}_2(\text{butyrate})_4$ ¹⁹ ($E_{1/2}$ values of +0.45, +0.30, and +0.39 V vs SCE), the $E_{1/2}$ values are

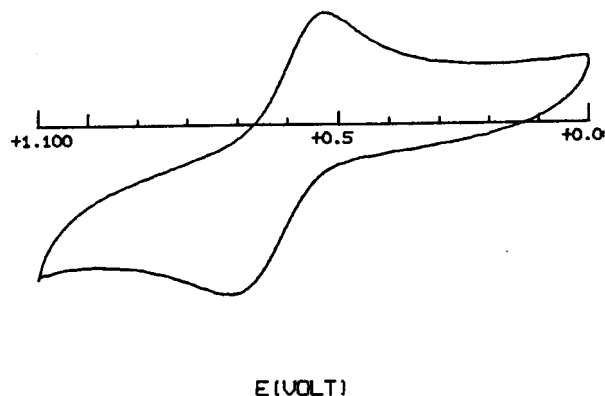


Figure 4. Cyclic voltammogram of tetrakis(2,4,6-triisopropylbenzoato)-dimolybdenum, **3**, in dichloromethane.

higher for **3** in all cases, when the difference in referencing procedures is taken into account. The cyclic voltammogram of $\text{Mo}_2(\text{O}_2\text{CCH}_3)_4$ in methanol is similar to that of compound **3**, with $E_{1/2} = +0.24$ V vs Ag/AgCl,²⁰ while measurements on solutions of $\text{Mo}_2(\text{pivalate})_4$ in acetonitrile and THF have $E_{1/2}$ values of +0.38 V vs SCE²¹ and +0.86 V vs Ag wire,²² respectively. These results contrast with those reported for $\text{Mo}_2(\text{aspirinate})_4$,²⁰ where an irreversible one-electron oxidation wave was observed. It is surprising that all of the noted compounds are more easily oxidized than **3**, yet no structures of the cations have been reported. To determine the reason for this gap in the literature, we sought to chemically oxidize another dimolybdenum carboxylate. We chose the pivalato derivative, $\text{Mo}_2(\text{O}_2\text{CC}_4\text{H}_9)_4$, due to its favorable solubility in dichloromethane and the presence of an electrochemically reversible oxidation wave ($\Delta E^\circ(\text{CH}_2\text{Cl}_2) = 0.133$ V), from which we determined $E_{1/2}(\text{CH}_2\text{Cl}_2) = 0.522$ V (vs Ag/AgCl). Although crystalline samples of $1 \cdot 2\text{CH}_2\text{Cl}_2$ and $2 \cdot 2\text{CH}_2\text{Cl}_2$ were obtained in moderate yield, according to eqs 1 and 2, we found that a similar oxidation of $\text{Mo}_2(\text{pivalate})_4$ provides green crystals of **4** only as a very minor product. Copious yellow and brown solids settle out of the dichloromethane solution when carefully layered with hexanes. Furthermore, these crystals are significantly less stable than those of $1 \cdot 2\text{CH}_2\text{Cl}_2$ and $2 \cdot 2\text{CH}_2\text{Cl}_2$ and lose crystallinity within a couple of days. After a great deal of effort, a crystal structure was obtained, Figure 5, with a Mo–Mo distance of 2.1512(5) Å, 0.063 Å longer than that in the parent compound.²³ Unfortunately, the low yield made bulk measurements impractical. It is also worth mentioning that the tetrabutyrato dimolybdenum cation has also been isolated.¹⁹ However, electrochemical experiments indicated that the cation was unstable, with a lifetime on the order of 1 min. Very likely the reason for the increased stability of the Mo_2^{5+} unit, when surrounded by the bulkier 2,4,6-triisopropylbenzoate anions,

(14) Cotton, F. A.; Frenz, B. A.; Webb, T. R. *J. Am. Chem. Soc.* **1973**, *95*, 4431.

(15) Cotton, F. A.; Timmons, D. J. *Polyhedron* **1998**, *119*, 7889.

(16) Cotton, F. A.; Daniels, L. M.; Liu, C. Y.; Murillo, C. A.; Wilkinson, C. *Angew. Chem., Int. Ed.*, submitted.

(17) Bailey, P. J.; Bone, S. F.; Mitchell, L. A.; Parsons, S.; Taylor, K. J.; Yellowlees, L. J. *Inorg. Chem.* **1997**, *36*, 867.

(18) Bailey, P. J.; Bone, S. F.; Mitchell, L. A.; Parsons, S.; Taylor, K. J.; Yellowlees, L. J. *Inorg. Chem.* **1997**, *36*, 5420.

(19) Cotton, F. A.; Pedersen, E. *Inorg. Chem.* **1975**, *14*, 399.

(20) Carvill, A.; Higgins, P.; McCann, G. M.; Ryan, H.; Shiels, A. *J. Chem. Soc., Dalton Trans.* **1989**, 2435.

(21) Santure, D. J.; Huffman, J. C.; Sattelberger, A. P. *Inorg. Chem.* **1985**, *24*, 371.

(22) (a) Cayton, R. H.; Chisholm, M. H.; Darrington, F. D. *Angew. Chem., Int. Ed. Engl.* **1990**, *29*, 1481. (b) Cayton, R. H.; Chisholm, M. H. *J. Am. Chem. Soc.* **1989**, *111*, 8921. (c) Cayton, R. H.; Chisholm, M. H.; Huffman, J. C.; Lobkovsky, E. B. *Angew. Chem., Int. Ed. Engl.* **1991**, *30*, 862.

(23) Cotton, F. A.; Extine, M.; Gage, L. D. *Inorg. Chem.* **1978**, *17*, 172.

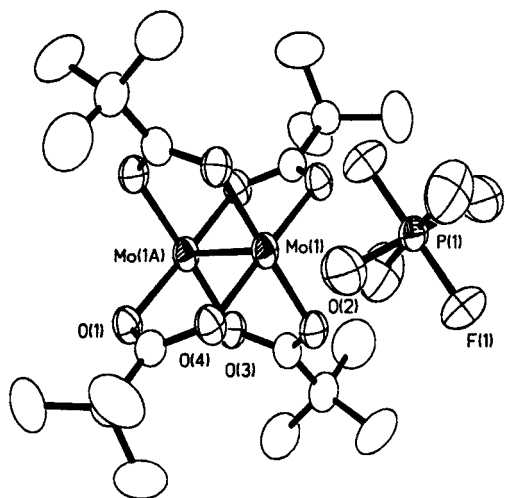


Figure 5. Thermal ellipsoid plot of the tetrakis(pivalato)dimolybdenum(II,III) cation and PF_6 anion in **4**. Probability ellipsoids are shown at the 50% level. Hydrogen atoms and disordered *tert*-butyl groups of minor occupancy have been omitted for clarity.

as compared to the less bulky pivalate or butyrate groups, is the capacity of the former to isolate the radical dimetal unit more effectively from the surrounding environment. This ability to tune the region of stability might be potentially useful for the exploitation of such units as one-electron oxidants for organic substrates. This is an area of great current interest²⁴ and where further work might prove rewarding.

The X-band (microwave frequency 9.42 GHz) EPR spectra of **1** and **2** in frozen dichloromethane at 70 K are consistent with a doublet ground state with both g_{\parallel} and g_{\perp} having the same value of 1.936. The spectra are similar to that reported for $[\text{Mo}_2(\text{O}_2\text{CC}_3\text{H}_7)_4]^+$, with $g_{\parallel} = g_{\perp} = 1.941$,¹⁹ and each may be interpreted in terms of the spin Hamiltonian (eq 4), with $S = 1/2$ and including species with nuclear spin states $I^1 + I^2 = J = 0, 5/2, \text{ and } 5$ with a natural abundance of 56%, 37.7%, and 6.3%, respectively.²⁵ We were not able to directly observe the 11-line pattern arising from the $J = 5$ isotopomer, likely due to poor instrument resolution. It should be pointed out that this small component is also not discernible in the simulation, although it has been added to our model at the appropriate natural abundance. The spin Hamiltonian parameters for **1** and **2** are listed in the caption to Figure 6 and are very similar to those reported for $\text{Mo}_2(\text{O}_2\text{CC}_3\text{H}_7)_4$.¹⁹

$$H = m[g_{\parallel}H_zS_z + g_{\perp}(H_xS_x + H_yS_y)] + A_{\parallel}S_z(I_z^1 + I_z^2) + A_{\perp}[S_x(I_x^1 + I_x^2) + S_y(I_y^1 + I_y^2)] \quad (4)$$

It may be noted that for the $[\text{Mo}_2(\text{HPO}_4)_4]^{3-}$ ion the g_{\parallel} and g_{\perp} were distinguishable (1.894, 1.866), but only barely.²⁶

The clear evidence of an unpaired electron from EPR spectroscopy provoked us to further investigate the magnetic properties of the cation, $[\text{Mo}_2(\text{TiPB})_4]^+$. Molar magnetic

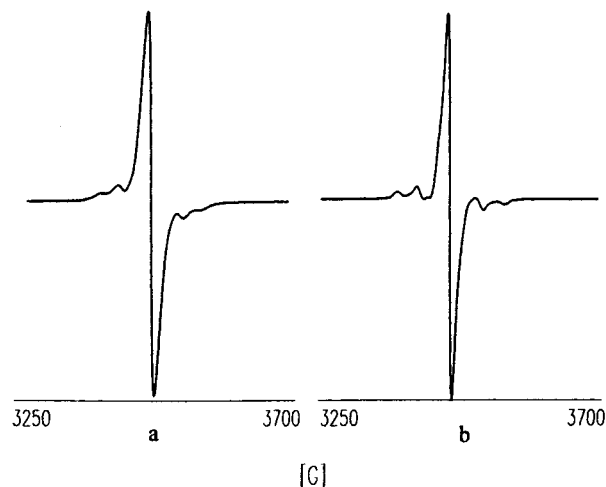


Figure 6. Electron paramagnetic resonance spectrum of **1** (a) and **2** (b) in frozen dichloromethane; $g_{\parallel} = g_{\perp} = 1.936$, $A_{\parallel} = 35.60 \times 10^{-4} \text{ cm}^{-1}$, and $A_{\perp} = 18.20 \times 10^{-4} \text{ cm}^{-1}$.

susceptibility measurements were carried out on crystalline samples of **2** using a SQUID magnetometer at 1000 G in the temperature range 300–2 K. The data for **2** were corrected for diamagnetic contribution by measuring the magnetic susceptibility of the neutral parent compound ($-0.0010 \text{ emu mol}^{-1}$). Compound **2** displays a linear $1/\chi$ plot, with the x -intercept very near zero (1.286 K), and a slope of 0.3474, as expected for a Curie paramagnet with $S = 1/2$. From eq 5, g was calculated to be 1.93, in rough agreement with the value extracted from the EPR data.

$$C = \frac{1}{8}g^2(S(S+1)) \quad (5)$$

The room temperature electronic spectrum for **1** shows three peaks: 550 ($\epsilon = 4700 \text{ M}^{-1} \text{ cm}^{-1}$), 365 ($\epsilon = 8400 \text{ M}^{-1} \text{ cm}^{-1}$), and 290 nm ($\epsilon = 10900 \text{ M}^{-1} \text{ cm}^{-1}$). The spectrum for **2** is quite similar, with peaks at 530 ($\epsilon = 4400 \text{ M}^{-1} \text{ cm}^{-1}$), 365 ($\epsilon = 8880 \text{ M}^{-1} \text{ cm}^{-1}$), and 290 nm ($\epsilon = 11100 \text{ M}^{-1} \text{ cm}^{-1}$). Compound **3** exhibits a poorly resolved shoulder at ca. 390 nm ($\epsilon = 13800 \text{ M}^{-1} \text{ cm}^{-1}$), a peak at 350 nm ($\epsilon = 22000 \text{ M}^{-1} \text{ cm}^{-1}$), and a shoulder at 290 nm ($\epsilon = 11400 \text{ M}^{-1} \text{ cm}^{-1}$). While the $\delta \rightarrow \delta^*$ transition in $\text{Mo}_2(\text{O}_2\text{CCR})_4$ complexes typically occurs at ca. 440 nm,¹ this region of the spectrum is obscured by what is a large, broad, presumably charge transfer band at 350 nm. It is tempting, albeit speculative, to assign the shoulder at ca. 390 nm to the $\delta \rightarrow \delta^*$ transition for two reasons. First, in light of the observation that axial ligands tend to lengthen the Mo–Mo bond, one expects the $\delta \rightarrow \delta^*$ transition to be at higher energy for the non-axially ligated compound **3**. Second, if we assign the lowest energy peak in **1** and **2** to the $\delta \rightarrow \delta^*$ transition, the difference in transition energy between the one-electron and two-electron systems is ca. 7300 cm^{-1} , a fair approximation of the exchange energy of quadruply bonded molybdenum compounds.²⁷ The large molar absorptivity coefficient of the putative $\delta \rightarrow \delta^*$ transition may be explained by significant mixing with the proximal, intense CT transition.

(24) See for example the review on the use of $\text{Fe}(\text{CN})_6^{3-}$ for the oxidation of organic substrates: Leal, J. M.; Garcia, B.; Domingo, P. L. *Coord. Chem. Rev.* **1998**, *173*, 79.

(25) Cotton, F. A.; Frenz, B. A.; Pedersen, E.; Webb, T. R. *Inorg. Chem.* **1975**, *14*, 391.

(26) Chang, I.-J.; Nocera, D. G. *J. Am. Chem. Soc.* **1987**, *109*, 4901.

(27) Cotton, F. A.; Nocera, D. G. *Acc. Chem. Res.* **2000**, *33*, 483.

The blue shift of the CT band in **3** from the 428 nm peak²⁸ exhibited by $\text{Mo}_2(\text{O}_2\text{CC}_6\text{H}_5)_4$ has been attributed to the twisting of the phenyl rings out of the CO_2 plane in the case of $\text{Mo}_2(\text{O}_2\text{C}(2,4,6\text{-Me}_3\text{C}_6\text{H}_2))_4$.²⁹ Likewise, in the centrosymmetric **3**, one phenyl blade is twisted 68° , while the other is twisted 34° from the carboxylate plane, thus disrupting the ligand conjugation and destabilizing the acceptor molecular orbital for a MLCT transition.

Conclusions

The first examples of dimolybdenum tetracarboxylato cations have been structurally characterized in $[\text{Mo}_2(\text{TiPB})_4]\text{PF}_6$, $[\text{Mo}_2(\text{TiPB})_4]\text{BF}_4$, and $[\text{Mo}_2(\text{O}_2\text{CC}_4\text{H}_9)_4]\text{PF}_6$. The crystal structures, EPR spectra, and electronic spectra all indicate that the lone electron resides in a metal-based δ orbital. While other $[\text{Mo}_2(\text{O}_2\text{CR})_4]^+$ complexes have been accessed via

(28) Chisholm, M. H.; Huffman, J. C.; Iyer, S. S.; Lynn, M. A. *Inorg. Chim. Acta* **1996**, *243*, 283.

(29) San Filippo, J., Jr.; Sniadoch, H. J. *Inorg. Chem.* **1976**, *15*, 2209.

reversible oxidation waves in solution, the 2,4,6-triisopropylphenyl carboxylato complexes exhibit far superior stability, and the three compounds whose structures are described here are the first and only ones that have been isolated and characterized fully.

Acknowledgment. We thank Dr. Huay-Keng Loke and Mr. Matthew Vogt for assistance with the EPR spectra, and Mr. Bradley W. Smucker and Mr. John F. Berry for assistance with magnetic measurements. We are grateful to the National Science Foundation for financial support. E.A.H. also thanks the NSF for a predoctoral fellowship.

Supporting Information Available: An X-ray crystallographic file in CIF format for compounds **1**·2 CH_2Cl_2 , **2**·2 CH_2Cl_2 , **3**, and **4**, and IR, NMR, and electronic spectra, magnetic susceptibility traces, cyclic voltammograms, and EPR simulations. This material is available free of charge via the Internet at <http://pubs.acs.org>.

IC011079R